Realistic $A=7$ hypernuclear productions

O. Richter, M. Sotona, and J. Žofka
Nuclear Physics Institute, Czechoslovak Academy of Sciences, 250 68 Řež, Prague, Czechoslovakia
(Received 26 November 1990)

Using large-basis realistic wave functions for ${}^{7}_{\Lambda}$Li (${}^{7}_{\Lambda}$He) hypernuclei, details of the production mechanisms in (K^-,π^-), (π^+,K^+), and (γ,K^+) processes are displayed, compared, and discussed. In particular, a selective but complementary population of different parts of spectra in these three reactions and a competition between the resolution and applicability of the realistic spectra are demonstrated. Different polarization abilities of the studied reactions are illustrated and optimal kinematical regions are sought, as well.

I. INTRODUCTION

An increased interest in novel hypernuclear (HY) productions and in particular in the electroproduction and photoproduction is encountered since recently. The reason for that is twofold: a progress of the Continuous Electron Beam Accelerator Facility (CEBAF) and a complementarity of the photoproduction reaction and other more "standard" hypernuclear productions. They populate different parts of spectra and only their sophisticated combination reveals the full complexity of the hypernuclear world. There are additional interests related to the detailed properties of the photoproduction process: The strong and complicated spin-flip part of the transition amplitude suggests a population of the spin-flip (upper) partners of doublets and a possibility of hypernuclear polarization. Low distortions are encountered in both incoming and outgoing beams; thus, a deep interior of hypernuclei is involved and tested, but not strongly disturbed. To really reveal these fine effects and their relative importance, a light nucleus (hypernucleus) with a rich structure described in a realistic model should be employed. One additional peculiarity of the strangeness photoproduction should be mentioned: There is not a single measurement existing on photoproduction of hypernuclei ($A>2$) and all the results for them are theoretical extrapolations from the elementary process to the multiparticle medium. In this respect, it would be highly desirable to have some experimental indication of nonelementary data before large machines start. At present, the theoretical predictions differ widely.

The first theoretical approaches to all three strangeness producing reactions dealt with simple targets (as, e.g., ^{12}C, ^{16}O, and ^{56}Fe) in an oversimplified particle-hole model and neglected the hypernuclear (HY) polarization. It is the aim of this work to use one and the same full model for all the three reactions on the target ^{7}Li, whose underlying (core) $A=6$ nuclei are complicated enough and they are treated realistically here. In fact, ${}^{7}_{\Lambda}$Li has already been studied in (K^-,π^-) reaction;[1,2] there is thus some testing material available. The model of (K^-,π^-) and (π^+,K^+) reactions has been recently developed so as to include the full amplitude and thus to encompass also the polarization.[3] The realistic description of photoproduction on targets of ^{12}C and ^{16}O has been proposed in Ref. 4. The alternative approach comparable with the model[3] and including also HY polarization can be found in Ref. 5. The latter one will be applied here. The reaction model is phenomenological, based on the existing data for the elementary reaction. It is that one used for (K^-,π^-) in Ref. 6, for (π^+,K^+) in Ref. 7, and proposed for (γ,K^+) in Ref. 5. In such a way, a fair comparison of all three processes is possible and their respective virtues may be appreciated. One of the novelties displayed here is the polarization attained in a complicated hypernucleus. The structure input is described in Sec. II, reactions are modeled in Sec. III, results and discussion are given in Sec. IV, followed by conclusions.

II. STRUCTURE OF ^{6}Li AND ${}^{7}_{\Lambda}$Li (${}^{7}_{\Lambda}$He)

The successful description of (K^-,π^-) production of ${}^{6}_{\Lambda}$Li in the translationally invariant shell model[8] (TISM) pointed at the possibility of its extension to the $A=7$ system. The ^{6}Li nuclear core underlying the latter is difficult for modeling. There are no bound ^{5}He or ^{5}Li nuclei on which ^{6}Li could be formed by simply adding a single nucleon. Also, ^{6}Li is not well accounted for by a hole in ^{7}Li. Nonetheless, the success in the description of ${}^{7}_{\Lambda}$Li (${}^{7}_{\Lambda}$He) depends critically on the correctness of the model for ^{6}Li.

The basis of TISM is used here. It is defined in terms of the internal degrees of freedom (in Jacobi coordinates):

$$|A\rho JT,nlj:\mathbb{J}\rangle=[|A-1\rho JT\rangle|nlj\rangle_{\Lambda}]^{\mathbb{J}} . \quad (1)$$

$|A-1\rho JT\rangle$ is a basis function for a description of $A-1$ nucleons. ρ stands for other quantum numbers needed for a unique classification. We use $0+1\hbar\omega$ shell-model space for $|A-1\rho JT\rangle$ (it is supposed that higher configurations do not contribute to the HY production on the target of ^{7}Li). $|nlj\rangle_{\Lambda}$ is the hyperon wave function. In this basis, we diagonalize the Hamiltonian

$$H=H_N+H_{\Lambda} , \quad (2)$$

where the nuclear part H_N is

$$H_N=\sum_{i=1}^{A-1}\frac{1}{2m_N}\left[p_i-\frac{1}{A-1}P_{A-1}\right]^2+\sum_{i<j}^{A-1}V_{NN}(r_i-r_j)\ , \tag{2a}$$

and that of the hyperon H_Λ is

$$H_\Lambda=\frac{\pi_\Lambda^2}{2\mu_\Lambda}+\sum_{i-1}^{A-1}V_{n\Lambda}(r_i-r_\Lambda)\ . \tag{2b}$$

Here, P_{A-1} is the total momentum of the nuclear core, π_Λ the momentum of the hyperon relative to that core, and μ_Λ is the corresponding reduced hyperon mass. The effective NN interaction of Ref. 9, fitted to all p-shell nuclei, is adopted here. This interaction reproduces, besides others, correctly the 2^-1 level of ^{6}Li at 21 MeV excitation, known experimentally and not fitted *a priori* in Ref. 9. The main component of this state is $|^{33}P_2[33](30)\rangle$ and it is essential in $s^{-1}s_\Lambda$ configurations. The single-particle energies relative to ^{4}He and ^{16}O cores, calculated in Ref. 9, reproduce the experimental data well. The harmonic-oscillator constant is chosen to be $b=2.04$ fm ($\hbar\omega_N=9.55$ MeV). For ^{6}Li, it gives the charge rms radius $\langle r_{\rm rms}\rangle_{\rm ch}=2.60$ fm, in agreement with the experimental value of 2.57 fm.[10] When the electron-scattering data on ^{6}Li were fitted by the one-body transition densities of valence nucleons,[11] a similar value of $b=2.03$ fm was obtained. The interaction of Ref. 9 predicts low-lying anomalous parity states of ^{6}Li, namely, the 2^-0 level at some 9 MeV excitation, with the configuration

$$0.88|^{13}P_2[42](30)\rangle\text{-}0.46|^{13}P_2[42](11)\rangle\ ,$$

which strongly affects the population of HY $p^{-1}p_\Lambda$ states.

To see further the influence of low-lying anomalous parity states of ^{6}Li on the shape of hypernuclear excitation function, the calculations here are also performed with the effective interaction of Ref. 12 [Eq. (13) therein, employed here for both normal and anomalous parity states]. To fix the 2^-1 level with the main component $|^{33}P_2[33](30)\rangle$ at the experimental value $E^*\sim 21$ MeV, $\hbar\omega_N=19.7$ MeV has to be chosen. Such an oscillator constant would not reproduce (e,e') scattering on ^{6}Li; nevertheless, it yields a reasonable single-particle splitting. The lowest 2^-0 level arises at some 13.6 MeV (and mixes only weakly into HY configurations $p^{-1}p_\Lambda$).

The effective ΛN interaction adopted here is that of Ref. 13,

$$V_{\Lambda N}=V(r)(1-\varepsilon+\varepsilon P_x)(1+\alpha\boldsymbol{\sigma}_N\cdot\boldsymbol{\sigma}_\Lambda)\ . \tag{3}$$

When using $\alpha=-0.1$, $\varepsilon=0$, and fitted Slater integrals $F^{(0)}=-1.16$ MeV, $F^{(2)}=-3.20$ MeV, $V_{\Lambda N}$ of Eq. (3) was successful in an interpretation of $p^{-1}p_\Lambda$ states. The above values for integrals $F^{(i)}$ were, however, fitted in the standard (translationally noninvariant) shell model as

$$\langle p(r_N)p(r_\Lambda):L|V_{\Lambda N}|p(r_N)p(r_\Lambda):L\rangle = F^{(0)}+F^{(2)}(\tfrac{1}{5}\delta_{L0}-\tfrac{2}{5}\delta_{L1}+\tfrac{1}{25}\delta_{L2})\ . \tag{4}$$

The $A=7$ system is too light and the use of TISM instead of the usual shell model is rather important in order to avoid the center-of-mass spuriosities. It can be shown,[14] however, that the same $p^{-1}p_\Lambda$ spectra are also obtained in TISM, if we change relation (4) as follows:

$$\text{RHS[Eq. (4)]}=\frac{A-1}{A-2}\langle p(\xi_N)p(\xi_\Lambda):L|V_{\Lambda N}|p(\xi_N)p(\xi_\Lambda):L\rangle-\frac{1}{A-2}\langle s(\xi_N)p(\xi_\Lambda):1|V_{\Lambda N}|s(\xi_N)p(\xi_\Lambda):1\rangle\ , \tag{5}$$

or

$$\text{RHS[Eq. (4)]}=\frac{A-1+x}{A-1}\langle p(r_N)p(r_\Lambda):L|V_{\Lambda N}|p(r_N)p(r_\Lambda):L\rangle-\frac{x}{A-1}\langle p(r_N)s(r_\Lambda):1|V_{\Lambda N}|p(r_N)s(r_\Lambda):1\rangle\ , \tag{6}$$

where RHS represents right-hand side. Equations (5) and (6) are equivalent and $F^{(i)}$ are not Slater integrals any more, but a suitable parametrization of the interaction (3). $\xi_N=R_{A-2}-r_N$ is the nucleon coordinate relative to the center of mass (c.m.) of the rest of the nuclear core ("$A-2$ core"); $\xi_\Lambda=R_{A-1}-r_\Lambda$ is the Λ hyperon coordinate relative to $(A-1)$ nuclear core, $x=m_\Lambda/m_N$. Equation (6) corresponds to the approach of Ref. 15. The radial dependence of the ΛN interaction has now to be fixed in order to calculate the matrix elements of the interaction (3) for other HY configurations ($p^{-1}s_\Lambda$ and $s^{-1}s_\Lambda$). The Gaussian form of $V_{\Lambda N}$ is chosen here:

$$V(r)=V_0e^{-(r/\rho)^2}\ . \tag{7}$$

Relation (5) [or (6)] yields $V_0=-16.8$ MeV and $\rho=1.72$ fm. Obviously, translationally noninvariant relation (4) would yield different V_0 and ρ (and, namely, $V_0=-26.2$ MeV and $\rho=1.42$ fm), but the spectra calculated in respective models for $p^{-1}p_\Lambda$ configurations are the same. They differ for other configurations. The harmonic-oscillator constant for hyperon $\hbar\omega_\Lambda$ was chosen so that the binding energy of the $\frac{1}{2}^+0$ ground state of $^7_\Lambda$Li is equal to the experimental value $B_\Lambda=5.58$ MeV, which yielded $\hbar\omega_\Lambda=10.5$ MeV. Such a value seems reasonable also from the comparison with, e.g., Ref. 16. Adopting now the above TISM values of V_0 and ρ, the scalar interaction for the configurations $p^{-1}s_\Lambda$ would be characterized by $\bar{V}=1.46$ and $\Delta=0.58$ (in notation of Ref. 17). Those values are in an acceptable agreement with the standard fitted set[17] $\bar{V}=1.49$, $\Delta=0.50$. Also the values V_0,ρ in the usual shell model yield plausible matrix elements $\bar{V}=1.38$ and $\Delta=0.55$. It should be mentioned in passing, however, that the nonexistence of the $M1$ transition in $^{10}_\Lambda$B ground-state doublet in the energy range

$E_\gamma=0.1-0.5$ MeV,[18] strongly supports a lower value of $\Delta\sim 0.3$ (and consequently a strong induced spin-orbit force $S_N\sim -0.3$).[19]

III. REACTION MODELS

The three HY production reactions compared here $[(K^-,\pi^-),(\pi^+,K^+),(\gamma,K^{+,0})]$ are all described in a similar way, keeping the relation to the amplitude of the elementary two-body process. The many-body aspects enter through kinematics, distortion, and wave functions of the underlying $A=6$ nucleus and resulting hypernucleus.

The distortion of incoming $\chi^{(+)}$ and outgoing $\chi^{(-)}$ meson waves is evaluated in the eikonal approximation. In the calculation of radial integrals $\langle\chi^{(-)}\psi_\Lambda|\chi^{(+)}\psi_N\rangle$, the harmonic-oscillator single-particle wave functions are reasonable for the deeply bound Λ-hyperon states. As in ${}^7_\Lambda$Li, the hyperon in the p state is barely bound or even unbound, it is simulated here by the Woods-Saxon single-particle p-wave functions corresponding to $B_\Lambda=0.1$ MeV. This procedure is frequently used in other nuclear reactions to get a more realistic description [e.g., $M1$ form factors in (e,e') scattering]. In the present case, the procedure outlined merely reduces the excitation strength as compared to that of harmonic oscillator.

The simple lines of the excitation function are smeared out and assume Breit-Wigner form with effective widths

$$\Gamma^{\text{eff}}=\sqrt{\Gamma^2+R^2}\ , \tag{8}$$

where Γ is the total width of the level, calculated in the R matrix theory from the strong hypernuclear decays. There, the TISM spectroscopic amplitudes are used and the Young schemes classification applied with advantage. R denotes the instrumental resolution. Widths (Γ's) calculated in this manner vary for the pronounced high-lying states between 1.5 and 7.7 MeV.

A good resolution allows for rich spectroscopy considerations. The precise energy splittings of HY states and their relative populations are primarily needed in verifying or fitting the effective ΛN interaction. A pronounced selectivity of polarization data and their information content makes them an ideal (though not always applicable in view of small cross sections) spectroscopic tool. They are reflected in the angular distributions of Λ-weak decay products and in Λ-magnetic moments measurements.

A. (K^-,π^-) in-flight reaction

The many-body laboratory cross section and polarization for this reaction are described in a standard way:[20,21]

$$\left.\frac{d\sigma}{d\Omega}\right|^{\text{lab}}=(2\pi)^4\frac{p_\pi^2E_KE_\pi E_H\overline{|T_{fi}|^2}}{p_K[p_\pi E_H+E_\pi(p_\pi-p_K\cos\theta_\pi)]}\ , \tag{9}$$

where

$$T_{fi}=\sqrt{A}\,\langle\Psi_H|\chi_\pi^{(-)}\langle\mathbf{p}_\pi\mathbf{q}|t|\mathbf{p}_K0\rangle_{\text{lab}}\chi_K^{(+)}|\Psi_A\rangle\ , \tag{10}$$

and

$$\overline{|T_{fi}|^2}=\frac{1}{(2J_A+1)}\sum_{M_AM_H}|T_{fi}|^2\ . \tag{11}$$

A,H denote the nuclear target and resulting hypernucleus, respectively. T_{fi} is the transition amplitude from the initial state of A to the final state of H, q is the momentum transferred. $\langle\ldots|t|\ldots\rangle$ is the elementary t matrix in the two-body laboratory system. Its two-body c.m. analog for the (K^-,π^-) reaction is taken from Ref. 6. The two-body c.m.→two-body laboratory (2c.m.→2lab) transformation of $\langle\ldots|t|\ldots\rangle$ is performed as in Ref. 20. The polarization of the produced hypernucleus is expressed as in Ref. 3,

$$P_{J_H}(\theta_\pi)=\frac{\sum_{M_H}M_H\sum_{M_A}|T_{fi}|^2}{(2J_A+1)J_H\overline{|T_{fi}|^2}}\ , \tag{12}$$

where the summation over the final-state projections M_H in Eq. (11) is replaced by the M_H weighted sum.

It was long believed that the spin-flip amplitude of the (K^-,π^-) reaction is negligible for $\theta_\pi\leq 30°$. The polarization ability of this reaction was thus not considered. However, the elementary reaction exhibits an enhanced polarization for kaon momenta above $p_K\geq 0.8$ GeV/c, as is demonstrated in Fig. 1 (reconstructed from amplitudes of Ref. 6). It is seen that the polarization is large in regions where the cross section is very small. Nonetheless, a transitive situation may be found (cross section still appreciable and polarization already noticeable) at $p_K\sim 0.905$ and $p_K\sim 1.1$ GeV/c. In fact, it has been demonstrated in Ref. 21 that on a nonelementary target (^{12}C) the HY polarization may be appreciable, as well.

B. (π^+,K^+) reaction

The description of this reaction proceeds in a full analogy with the (K^-,π^-) in-flight reaction, as described in the preceding paragraph. Two recent studies[3,22] are de-

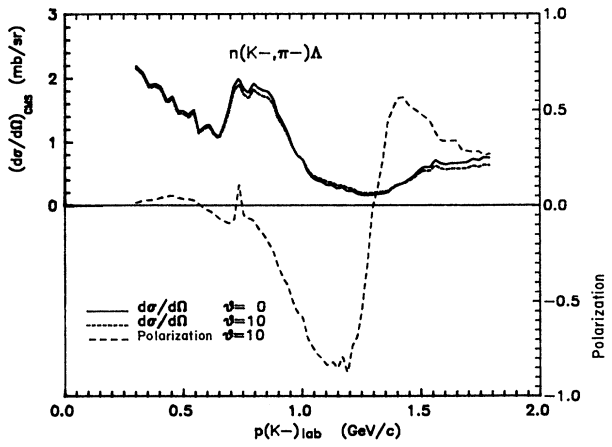

FIG. 1. Elementary c.m. cross sections and polarizations for the reaction $n(K^-,\pi^-)\Lambda$ at various angles of outgoing meson and various incident momenta.

voted to the (π^+,K^+) reaction details and the review[21] compares it with others throughout, thus there is no need to repeat all the arguments. The elementary t matrix is taken as parametrized in Ref. 7. The 2c.m.$\rightarrow$2lab transformation is again that of Ref. 20. The formulas for the cross section and polarization are those of Eqs. (9) and (12); the quantities referring to π and K mesons are interchanged only.

The (π^+,K^+) reaction is characterized by the threshold (around 0.65 GeV/c for the heaviest targets), large transferred momenta ($\geq$0.35 GeV/c), smaller cross sections ($\sim$few tens of microbarns), and an appreciable spin-flip amplitude leading to a large polarization.[3] Noticeable of this reaction is its pronounced selectivity, which provides a separated series of peaks, corresponding to valence nucleon holes and Λ in all orbits with maximum momentum transferred ($L=l_n+l_\Lambda$).

The main features of the elementary cross section are displayed in Fig. 2. Strong p_K dependence and selective angular behavior can be revealed there.

C. HY photoproduction

After preliminary considerations in the early 1970's,[23] the HY photoproduction has been actively pursued by as much as five different groups.[4,24–27] They construct the photoproduction amplitude based on diagrammatic techniques. Including various graphs, more or less involved amplitudes of the elementary process $(\gamma N\rightarrow\Lambda K)$ are obtained. However, further adjustments are found to be necessary by comparison with the experimental data (on differential and total cross sections and some on polarizations).

In order to construct the amplitude, we have adopted consistently a phenomenological approach here. It was sketched shortly before[5] and it is analogous to Secs. III A and III B. The elementary amplitude is taken from Ref. 28. In contrast to the (K^-,π^-) and (π^+,K^+) processes, it contains three spin-flip amplitudes:

$$F^{\text{2c.m.}}=iF_1(\boldsymbol{\sigma}\cdot\hat{\boldsymbol{\varepsilon}})+F_2(\boldsymbol{\sigma}\cdot\hat{\mathbf{q}})(\boldsymbol{\sigma}\cdot[\hat{\boldsymbol{\kappa}}\times\hat{\boldsymbol{\varepsilon}}])$$
$$+iF_3(\boldsymbol{\sigma}\cdot\hat{\boldsymbol{\kappa}})(\hat{\mathbf{q}}\cdot\hat{\boldsymbol{\varepsilon}})+iF_4(\boldsymbol{\sigma}\cdot\hat{\mathbf{q}})(\hat{\mathbf{q}}\cdot\hat{\boldsymbol{\varepsilon}})\ . \tag{13}$$

Here, $\boldsymbol{\sigma}$ is the baryon Pauli matrix, $\hat{\boldsymbol{\varepsilon}}$ the photon polarization, $\hat{\boldsymbol{\kappa}}$ ($\hat{\mathbf{q}}$) are in (out) 2c.m. momenta, and $\hat{\mathbf{x}}=\mathbf{x}/x$. F_i are functions of q,κ and of the scattering angle. To transform the 2c.m. t matrix into the two-body laboratory system, where

$$\langle\mathbf{p}_K,\mathbf{k}_\gamma-\mathbf{p}_K|t|\mathbf{k}_\gamma 0\rangle=iA_1(\boldsymbol{\sigma}\cdot\hat{\boldsymbol{\varepsilon}})+iA_2(\boldsymbol{\sigma}\cdot\hat{\mathbf{k}}_\gamma)(\hat{\mathbf{p}}_K\cdot\hat{\boldsymbol{\varepsilon}})$$
$$+iA_3(\boldsymbol{\sigma}\cdot\hat{\mathbf{p}}_K)(\hat{\mathbf{p}}_K\cdot\hat{\boldsymbol{\varepsilon}})$$
$$+A_4([\hat{\mathbf{k}}_\gamma\times\hat{\mathbf{p}}_K]\cdot\hat{\boldsymbol{\varepsilon}})\ , \tag{14}$$

transformation matrix λ^i_j can be used. We write it explicitly in the Appendix. The expressions for $d\sigma/d\Omega$ and P are derived in Ref. 5 and are similar to Eqs. (9) and (12). Here, however, the additional averaging over the photon polarization $\hat{\boldsymbol{\varepsilon}}$ arises. The photoproduced HY polarization has also been studied[29] recently.

The transferred momentum ($q\sim$0.28 GeV/c at $\theta_K=0°$) of this reaction is comparable to that of the (π^+,K^+) one and also the thresholds are similar ($p_\gamma^{\text{th}}=0.911$ GeV/c for the elementary reaction and 0.710 GeV/c for that on ^{7}Li target).

The production of strangeness via the electroproduction $(e,e'K^+)$ is qualitatively similar. In this case, it is mediated by the virtual photon. If the latter is not too far from the mass shell, both photoproduction and electroproduction are very close for the same photon energy. In addition, a very good resolution ($R<1$ MeV) is expected for both processes at the multi-GeV facility CEBAF.[30]

The angular and momenta dependence of the elementary (γ,K^+) amplitude is depicted in Fig. 3.

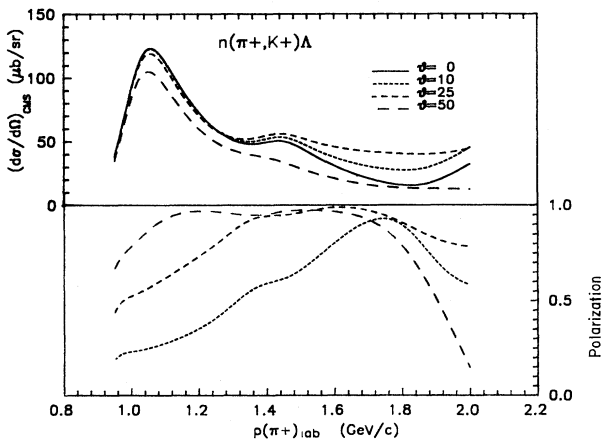

FIG. 2. Elementary c.m. cross sections and polarizations for the reaction $n(\pi^+,K^+)\Lambda$ at various angles of outgoing meson and various incident momenta.

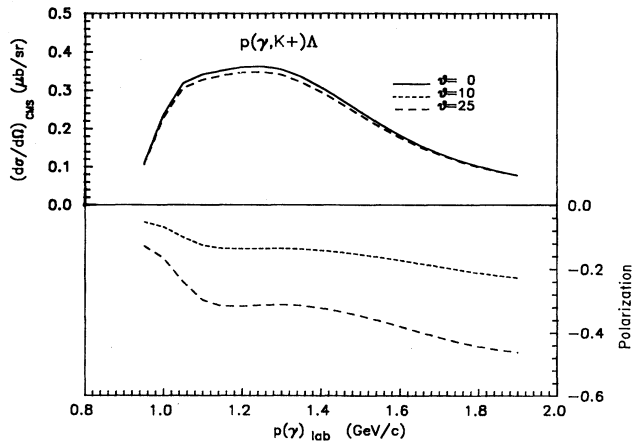

FIG. 3. Elementary c.m. cross sections and polarizations for the reaction $p(\gamma,K^+)\Lambda$ at various angles of outgoing meson and various incident momenta. (The curve for the cross section at $\theta_K=10°$ coincides with that at $\theta_K=0°$.) The phenomenological amplitude here and further on in hypernuclear (γ,K) calculations is that of Ref. 28 (denoted as 6b there).

IV. RESULTS AND DISCUSSION

A. (K^-,π^-) in-flight production of $^7_\Lambda$Li

In view of the specific properties of this reaction, one may expect the excitation function with two strong peaks (substitutional states; large sticking caused by a low transfer at small angles of outgoing pions). And indeed, in the earlier experiments,[1] the spectrum of $^7_\Lambda$Li was taken at $p_K=720$ (790) MeV and two pronounced peaks at $E_\Lambda=2.7$ and 14.6 MeV have been observed (see Fig. 4). Here and further on $E_\Lambda=-B_\Lambda$. The small peak observed at $E_\Lambda=-5.6$ MeV has been ascribed to the ground state of $^7_\Lambda$Li.

When interpreting the $^7_\Lambda$Li spectrum theoretically, the use of the Van Hees NN interaction[9] leads to an identification of the lower major peak at 2.7 MeV with three $|\frac{3}{2}^-0\rangle$ states, which are strong mixtures of configurations $p^{-1}p_\Lambda$ and $s^{-1}s_\Lambda$ (see Fig. 4). In particular, states obtained at $E_\Lambda=2.8$, 3.9, and 4.6 MeV are mixtures of configurations $|E_{\text{g.s.}},1^+0\rangle|p^j_\Lambda\rangle$, $|2.18$ MeV,$3^+0\rangle|p^{3/2}_\Lambda\rangle$, and $|9.0$ MeV, $2^-0\rangle|s_\Lambda\rangle$. These HY states cannot be experimentally distinguished due to their large decay widths (some 5 MeV) especially into ^{6}Li$+\Lambda$ and $^5_\Lambda$He$+d$ channels.

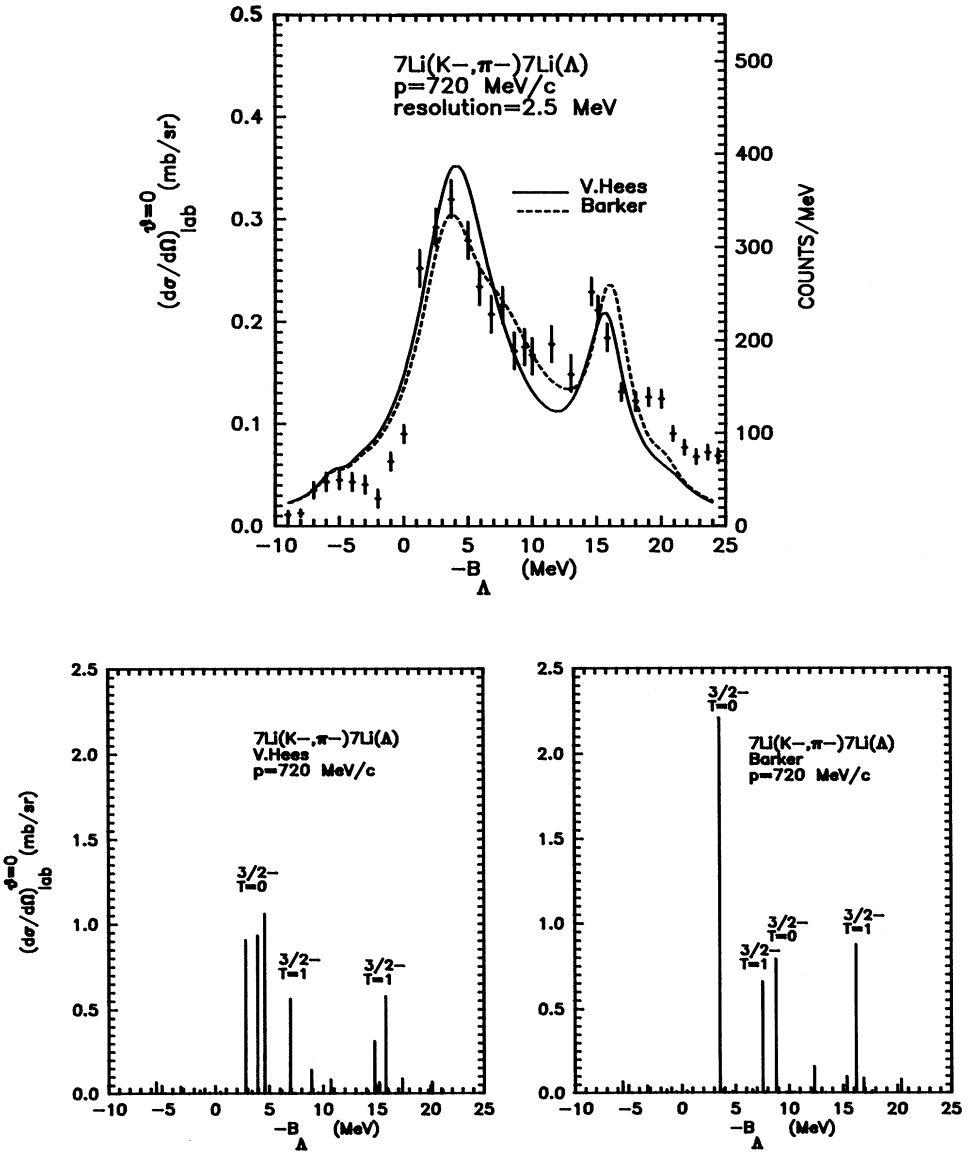

FIG. 4. The excitation functions for the reaction ^{7}Li$(K^-,\pi^-)^7_\Lambda$Li at $p_K=720$ MeV/c, resolution $R=2.5$ MeV, and $\theta_\pi=0°$ (collinear geometry). Theoretical smoothed curves and line spectra are given for two NN interactions (Refs. 9 and 12); spin-isospin assignments are indicated. The experimental excitation function (Ref. 1) is rescaled to the height of the first peak (factor 0.8 transforms the left scale to the right one).

It should be mentioned that a restriction to the configurations $p^{-1}p_\Lambda$ only would yield a single strongly excited state $|\frac{3}{2}^-0\rangle$ at the energy $E_\Lambda=3.4$ MeV (width $\Gamma=4.5$ MeV).

The Barker NN interaction[12] splits strongly states of normal and anomalous parity in ^{6}Li. Indeed, it gives the lowest anomalous parity 2^-0 level as high as at 13.6 MeV excitation. Consequently, the configurations $p^{-1}p_\Lambda$ and $s^{-1}s_\Lambda$ are not strongly mixed. The $|\frac{3}{2}^-0\rangle$ state at $E_\Lambda=3.5$ MeV, having the configuration $p^{-1}p_\Lambda$, is populated prominently, whereas another $|\frac{3}{2}^-0\rangle$ state at $E_\Lambda=8.7$ MeV (with the structure $s^{-1}s_\Lambda$ and a large decay width $\Gamma=7.7$ MeV into nucleon, deuteron, and α channels) gets less strength. Their separate identification would be again difficult although some enhancement in the region of $E_\Lambda\sim 8$ MeV may be noticed in the experiment.[1]

The information on the low-lying states of ^{6}Li (underlying the interpretation of $^7_\Lambda$Li) is obtained from the elastic scattering of d on ^{4}He. Broad resonances $|^{13}P_J[42]\rangle$ of anomalous parity should be traced in the corresponding phase shifts. However, no such states (low-lying ones at around 9 MeV or high-lying ones at some 13 MeV) were found experimentally.

Other models approached the lower peak as follows: The cluster model[31] yielded a peak at $E_\Lambda=3.1$ MeV; the configurations $s^{-1}s_\Lambda$ were not included there, however. The shell model with $p^{-1}(nl)_\Lambda$ configurations[15] generated a peak at $E_\Lambda=3.4$ MeV, whereas, that of Ref. 32, including $s^{-1}s_\Lambda$ configurations (nuclear 2^-0 level at $E^*=12$ MeV there), led to the state at $E_\Lambda=4.8$ MeV.

The second major peak of the excitation function is identified with the $|\frac{3}{2}^-1\rangle$ state at $E_\Lambda=16.1$ MeV, $\Gamma=2.2$ MeV (Barker interaction) or at $E_\Lambda=15.8$ MeV, $\Gamma=2.0$ MeV (Van Hees interaction). The configuration $|21.0$ MeV, $2^-1\rangle|s_\Lambda\rangle$ dominates in it. The underlying nuclear 2^-1 level itself has mainly $|^{33}P_2[33]\rangle$ structure and possesses a large spectroscopic amplitude for the s-nucleon knockout off the target ^{7}Li. Consequently, in order to explain a broad bump in $(p,2p)$ reactions on ^{7}Li (seen at some 13–16 MeV excitation in ^{6}He), the corresponding 2^-1 level in ^{6}Li is sometimes artificially shifted by 3 MeV down.[33] However, such a shift would be reflected by a much lower $|\frac{3}{2}^-1\rangle$ state in the HY spectrum of $^7_\Lambda$Li. The position of the latter thus tests the nuclear single-particle energy ε_s.

The HY second major peak may serve also as a sensitive test of the wave function of the nuclear 2^-1 level and, consequently, of the NN interaction. To demonstrate this fact, let us express the excitation energy of the $|\frac{3}{2}^-1\rangle$ state in terms of main components only:

$$\begin{aligned}E^*_{\rm th}(^7_\Lambda{\rm Li})&=E_\Lambda(\tfrac{3}{2}^-1)-E_\Lambda({\rm g.s.};\tfrac{1}{2}^+0)\\&=E(^{33}P_2[33]\times s_\Lambda:\tfrac{3}{2}^-1)-E(^{13}S_1[42]\times s_\Lambda:\tfrac{1}{2}^+0)\\&=21.0-[\bar V+\langle s_Ns_\Lambda|V_0|s_Ns_\Lambda\rangle]+\tfrac{3}{8}[\Delta-\langle s_Ns_\Lambda|V_\sigma|s_Ns_\Lambda\rangle]+\tfrac{1}{4}\Delta+\tfrac{1}{6}S_N-\tfrac{3}{4}S_\Lambda+\tfrac{27}{50}T\ ,\end{aligned}\tag{15}$$

in parametrization of Ref. 17. For estimating the interaction of Λ and N in s states, the position of the analogous $s^{-1}s_\Lambda$ peak in $^6_\Lambda$Li at $E_\Lambda=18.3$ MeV may be used.[8] That $|1^+\tfrac{1}{2}\rangle$ state has the pronounced dominant component $|16.66$ MeV, $\frac{3}{2}^+\frac{1}{2}\rangle|s_\Lambda\rangle$. The underlying nuclear $\frac{3}{2}^+$ level, in contrast to the analogous ^{6}Li one, is a very sharp resonance with $|^{24}S_{3/2}[32](20)\rangle$ structure:

$$\begin{aligned}E^*_{\rm th}(^6_\Lambda{\rm Li})&=E_\Lambda(1^+\tfrac{1}{2})-E_\Lambda({\rm g.s.};1^-\tfrac{1}{2})=18.3\\&=E(^{24}S_{3/2}[32]\times s_\Lambda:1^+\tfrac{1}{2})-E(^{22}P_{3/2}[41]\times s_\Lambda:1^-\tfrac{1}{2})\\&=16.7-[\bar V+\langle s_Ns_\Lambda|V_0|s_Ns_\Lambda\rangle]+\tfrac{5}{12}[\Delta-\langle s_Ns_\Lambda|V_\sigma|s_Ns_\Lambda\rangle]-\tfrac{10}{12}\Delta-\tfrac{1}{2}S_N+\tfrac{5}{6}S_\Lambda-T\ .\end{aligned}\tag{16}$$

The term $\Sigma=\Delta-\langle s_Ns_\Lambda|V_\sigma|s_Ns_\Lambda\rangle$ is small. For example, by fixing the radial dependence of V_σ in the Gaussian form, we obtain $\Sigma\approx-\Delta/2$. Taking into account also small coefficients at Σ, both in Eqs. (15) and (16), we can safely neglect its contribution. So by comparing Eqs. (15) and (16), for the excitation energy of the $|\frac{3}{2}^-1\rangle$ state in $^7_\Lambda$Li, it holds:

$$E^*_{\rm th}(^7_\Lambda{\rm Li})=22.6+\tfrac{13}{12}\Delta+\tfrac{2}{3}S_N-\tfrac{19}{12}S_\Lambda+\tfrac{77}{50}T\ .\tag{17}$$

Hence, independently of the particular ΛN interaction (S_N, S_Λ, T are small and $\Delta>0$, anyway), it follows here for the excitation energy of the $|\frac{3}{2}^-1\rangle$ state derived above:

$$E^*_{\rm th}(^7_\Lambda{\rm Li})>E^*_{\rm exp}=14.6-(-5.6)=20.2\ {\rm MeV}\ .\tag{18}$$

In other words, assuming the nuclear 2^-1 level as pure $|^{33}P_2[33]\rangle$ configuration, the HY $|\frac{3}{2}^-1\rangle$ state will lie too high. Consequently, the position of this peak in $^7_\Lambda$Li may serve as a test of small components in the wave function of the nuclear 2^-1 level (and of the underlying NN interaction). This is a remarkable property as this nuclear state itself is a very broad resonance (due to the decay channel ^{3}H+^{3}He).

The collinear geometry ($\theta_\pi=0°$) is not a good instrument for getting detailed information on the bound states of $^7_\Lambda$Li. If, however, pions at $\theta_\pi=10°$ are taken with resolution of $R=1$ MeV, bound low-lying states appear as

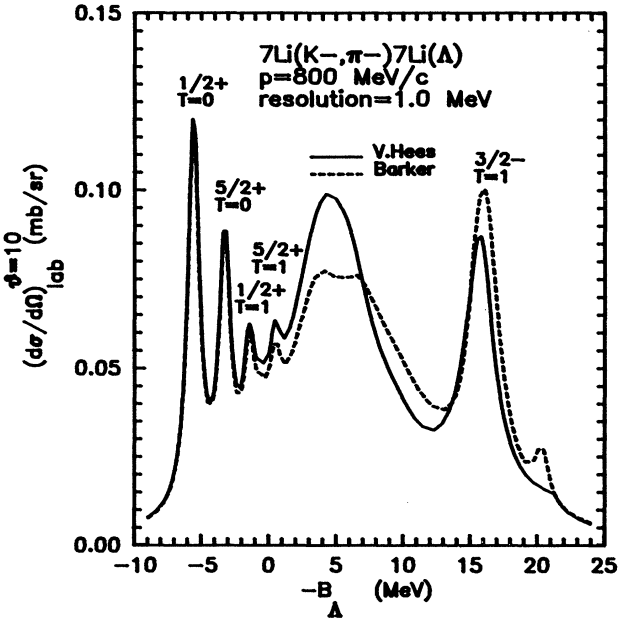

FIG. 5. The excitation function $^7\mathrm{Li}(K^-,\pi^-)^7_\Lambda\mathrm{Li}$ at $p_K=0.8$ GeV/c, $\theta_\pi=10°$, and high-quality resolution $R=1.0$ MeV.

sharp separate peaks (Fig. 5). Those are $|\frac{1}{2}^+0\rangle$ ground state, $|\frac{5}{2}^+0\rangle$ state at $E_\Lambda=-3.25$ MeV, $|\frac{1}{2}^+1\rangle$ at $E_\Lambda=-1.43$ MeV, and $|\frac{5}{2}^+1\rangle$ at $E_\Lambda=0.47$ MeV, as obtained here theoretically. Experimentally,[34] by measuring the HY γ quanta in $^7_\Lambda$Li, $E_\gamma(\frac{5}{2}^+\rightarrow\frac{1}{2}^+)=2.03$ MeV was found. The slightly larger theoretical value here ($E_\gamma=2.33$ MeV) stems from the scalar character of the standard ΛN interaction[13] used (neglecting the induced spin-orbit force S_N).

It is interesting that the relative height of HY peaks at $E_\Lambda\sim4$ and 15 MeV is rather sensitive to the NN interaction used for $\theta_\pi>0°$. With the increasing π-detection angle, the strength of the pure $p^{-1}p_\Lambda$ configurations decreases faster than those with $s^{-1}s_\Lambda$ (the radial integrals $\langle\chi^{(-)}\Psi_\Lambda|\chi^{(+)}\Psi_N\rangle$ depend on the momentum transfer). Consequently, the strong mixture $p^{-1}p_\Lambda+s^{-1}s_\Lambda$ for Van Hees interaction is less extensively reduced with an increasing angle than that of $p^{-1}p_\Lambda$ for Barker interaction. The relative population strength of both $\frac{3}{2}^-$ substitutional states can thus prove or eliminate the existence of the low-lying anomalous parity states in ^{6}Li.

As proposed in Ref. 35, the enhanced polarization is encountered even for the reaction (K^-,π^-) in flight. This is demonstrated here in Fig. 6, displaying the excitation function of $^7_\Lambda$Li at $\theta_\pi=10°$ for K mesons with $p_K=905$ MeV/c. However, highly polarized states are not strongly populated with the exception of the $|\frac{5}{2}^+0\rangle$ state ($P=0.22$) and the $|\frac{1}{2}^+1\rangle$ state ($P=-0.43$), which are both polarized and fed strongly. As expected from Fig. 1, when further increasing p_K to the value of $p_K=1100$ MeV/c, polarizations at $\theta_\pi=10°$ reach remarkable values approaching often unity [$P(\frac{1}{2}^+0)=0.58$,

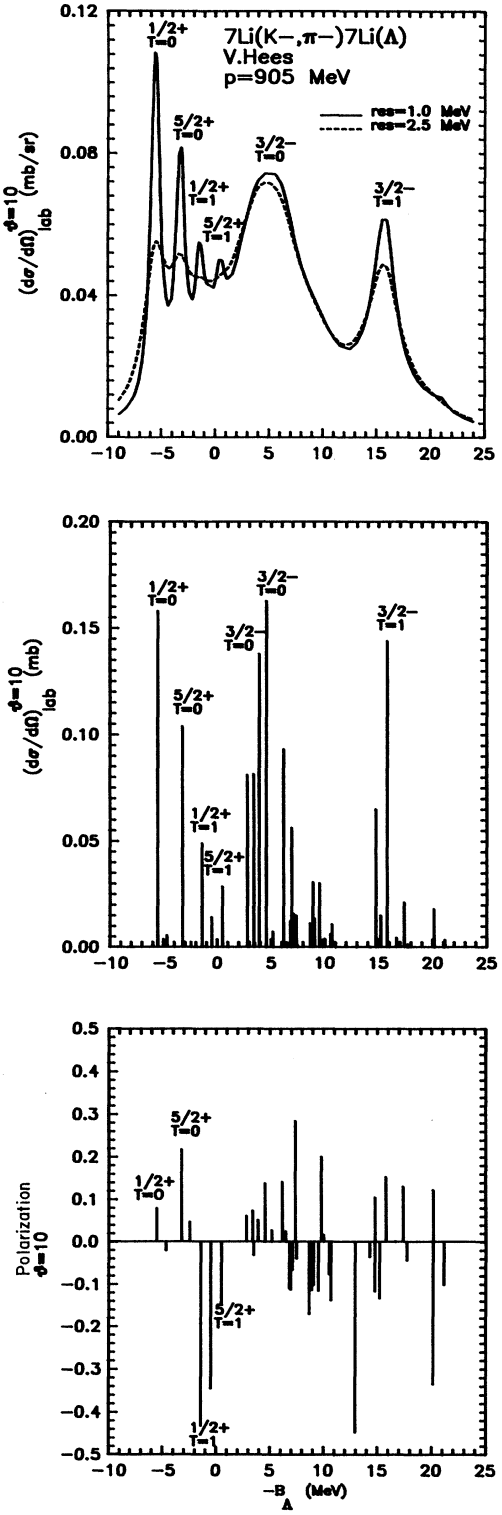

FIG. 6. The excitation functions and polarization for the reaction $^7\mathrm{Li}(K^-,\pi^-)^7_\Lambda\mathrm{Li}$ at $\theta_\pi=10°$ two resolutions and $p_K=0.905$ GeV/c (polarizing region). Polarizations have spin-isospin indication for appreciably populated states only; calculations here and further on have been performed with the NN interaction of Ref. 9.

$P(\frac{1}{2}^+1)=-0.99$, $P(\frac{5}{2}^+1)=-0.70$]. The above discussed resonance $|\frac{3}{2}^-1\rangle$ (at $E_\Lambda^{\exp}=+14.6$ MeV) assumes then as much as $P=0.58$ polarization.

The differential cross section summed over all states calculated here amounts to 4.3 mb/sr for the Woods-Saxon wave function (4.8 mb/sr for the harmonic-oscillator ones) and it is in good agreement with the experimental value[1] of 4.4±1.2 mb/sr for $p_K=790$ MeV/c.

B. (π^+,K^+) production of $^7_\Lambda$Li

The inspection of the elementary reaction cross section (Ref. 7 and Fig. 2) suggests $p_\pi\sim1.05$ GeV/c as the most efficient momentum for the HY production. The large cross sections at $\theta_\pi=0°$ and large transferred momentum allow us to expect a sufficient population of high-spin states and $\Delta l=1$ $p^{-1}s_\Lambda$, $\Delta l=2$ $p^{-1}p_\Lambda$ transitions. An appreciable elementary spin-flip amplitude in the region of momenta of interest points at the production of an enhanced polarization and population of both natural and non-natural states. Analysis of the amplitude, however, shows that population of only one member of the doublet prevails and the reaction (π^+,K^+) alone is not able to reveal clearly the (small) spin splitting of low-lying $(p^{-1}s_\Lambda)$ HY states.

This all is clearly illustrated in the calculated excitation functions and polarizations of $^7_\Lambda$Li in Figs. 7 and 8. In the collinear setup ($\theta_K=0°$), the low-lying states $|\text{g.s.},\frac{1}{2}^+0\rangle$ and $|2.33\text{ MeV},\frac{5}{2}^+0\rangle$ are strongly excited and are seen as separate peaks even with a bad resolution $R=2.5$ MeV. When improving the resolution also states $|\frac{1}{2}^+1\rangle$ and $|\frac{5}{2}^+1\rangle$ become visible. This is the same group of states, distinguished in the (K^-,π^-) reaction (Sec. IV A), but there at $\theta_\pi=10°$, thus at the decreased efficiency. For the (π^+,K^+) reaction, the excitation function does not change so dramatically when increasing the angle of the outgoing meson from $\theta_\pi=0°$ to 10° (cf. upper parts of Figs. 7 and 8), the reason being much smaller relative change of the transferred momentum [350 to 380 MeV/c as compared with 50 to 100 MeV/c in the case of (K^-,π^-) reaction]. The cross sections decrease by a factor of 2 approximately when changing θ_K from 0° to 10°, but the polarization appears in addition (the bottom lowest part of Fig. 8).

The group of states is also strongly excited around $E_\Lambda\sim5$ MeV, namely, $|\frac{3}{2}^-0\rangle$, $|\frac{1}{2}^-0\rangle$, and $|\frac{7}{2}^-0\rangle$. Similarly, as in the case of the (K^-,π^-) reaction, they are $p^{-1}p_\Lambda$ configurations (a mixture with $s^{-1}s_\Lambda$ for $|\frac{3}{2}^-0\rangle$ state). They have very different relative weights, with preponderance of the relatively narrow ($\Gamma=3.0$ MeV) stretched $|\frac{7}{2}^-0\rangle$ state. Those with lower spins have large decay widths $\Gamma\sim5.0$ MeV and cannot be thus identified as separate peaks.

The upper peak (prevailingly $|\frac{3}{2}^-1\rangle$ state) at $E_\Lambda\sim15$ MeV is less appreciably populated than in the (K^-,π^-) process. This is mainly due to the difference in the transferred momentum and the $s^{-1}s_\Lambda$ character of that group.

A changed kinematics (increased momentum) does not change the shape of the excitation function significantly, but the absolute values differ. In particular, at $p_\pi=1.5$ GeV/c, the cross sections decrease by a factor of 3–5, but polarization increases almost twice (reaching values close to 1 for some states). When compared with the cluster calculation,[36] the agreement is fair; however, the states around $E_\Lambda=5$ MeV are more emphasized here than in Ref. 35.

C. Photoproduction of $^7_\Lambda$Li ($^7_\Lambda$He)

This reaction is a useful complement to the above two processes. It has a similar kinematics (large momentum transfer) with the (π^+,K^+) reaction. Pronounced spin-

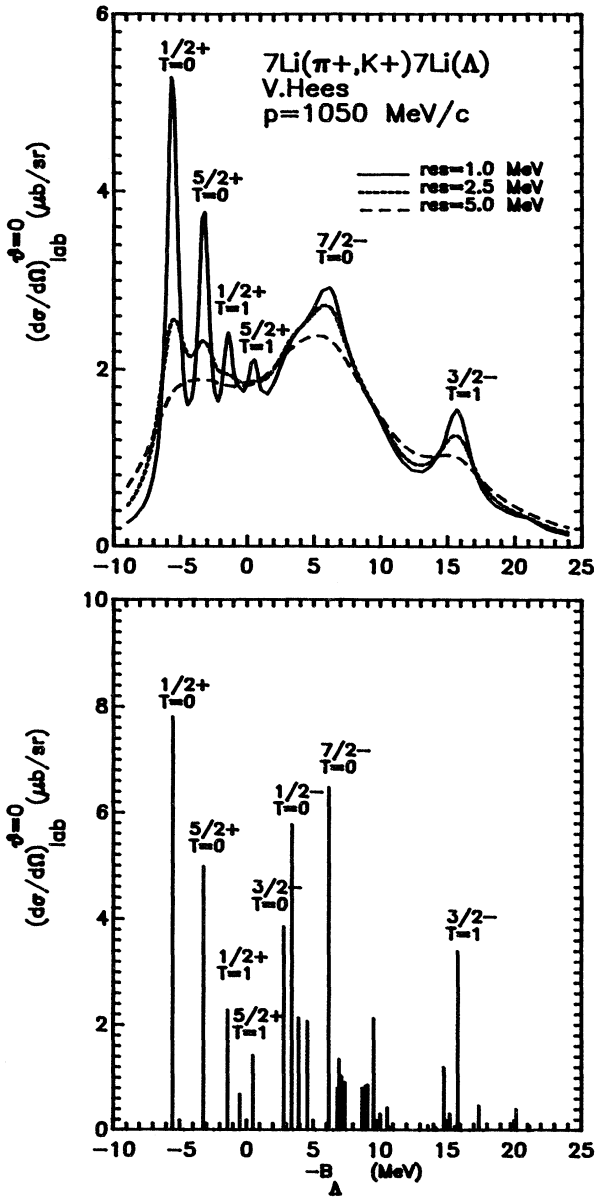

FIG. 7. The excitation functions for the reaction ^{7}Li$(\pi^+,K^+)^7_\Lambda$Li at $p_\pi=1.05$ GeV/c, $\theta_K=0°$, and three resolutions $R=1.0$, 2.5, and 5.0 MeV.

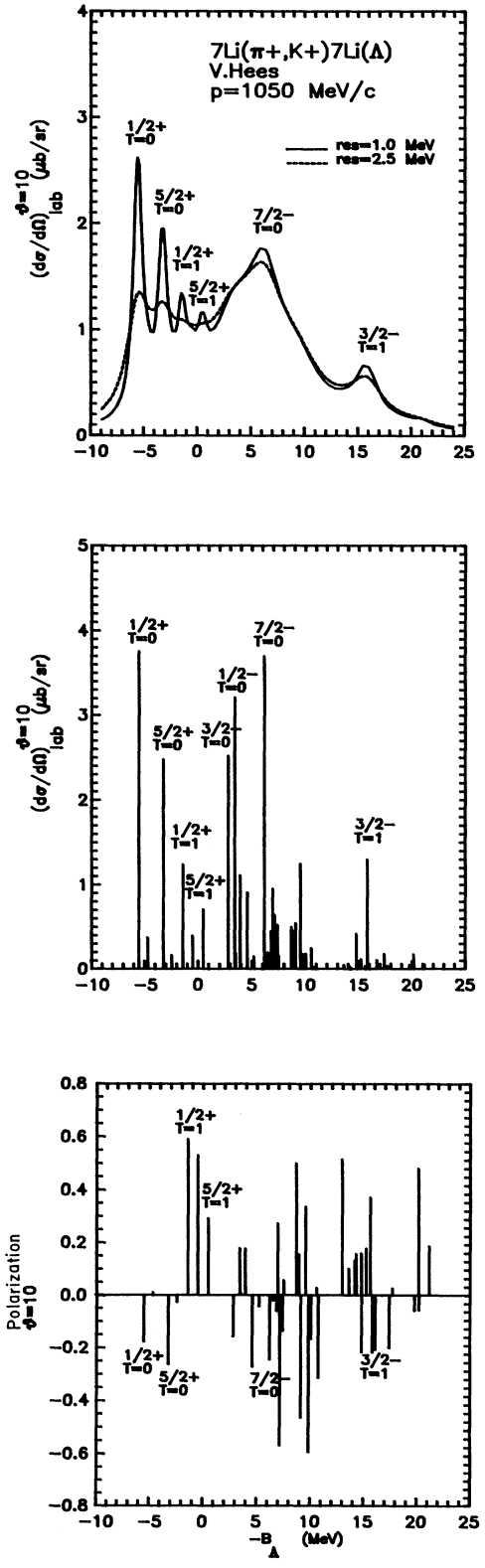

FIG. 8. The excitation functions and polarization for the reaction $^{7}\mathrm{Li}(\pi^{+},K^{+})^{7}_{\Lambda}\mathrm{Li}$ at $p_{\pi}=1.05$ GeV/c, $\theta_{K}=10°$, and $R=1.0$ and 2.5 MeV. Strongly excited and polarized states are indicated by spin-isospin assignments.

flip amplitudes excite comparably both natural and nonnatural parity states. It makes the photoproduction a suitable tool for studying low-lying doublets and polarizations (the elementary differential cross section at 1.2 GeV reaches some 0.3 μb/sr at $\theta_{K}\sim 0°-30°$; see Fig. 3). Another important spectroscopic virtue of the photoproduction is a relatively weak interaction of K^{+} meson and photon γ with the nuclear medium. K^{+} has mean free path of about 7 fm in the nuclear medium and may map a deep interior of it.

A first inspection of the photoproduction excitation function reveals that even at an intermediate resolution of $R=5$ MeV, three similarly pronounced peaks are seen. Their relative intensity varies with p_{γ} (upper part of Fig. 9) and with various parametrizations of the elementary amplitudes. Only when the resolution exceeds the value of 10 MeV, three peaks start to combine into a single broad resonance which would nonetheless give a rough estimate of the summed nonelementary cross section. The latter, amounting to 2 μb/sr at $\theta_{K}=0°$ and $p_{\gamma}=1.2$ GeV/c in the theoretical model, is completely lacking in a list of experimental HY data, as yet.

The lowest peak (Fig. 9) corresponds to the excitation of the ground state of $^{7}_{\Lambda}\mathrm{He}$ ($E_{\Lambda}=-5$ MeV, $\frac{1}{2}^{+}1$); the middle one at $E_{\Lambda}\sim 5$ MeV includes states $|\frac{3}{2}^{-}1\rangle$, $|\frac{7}{2}^{-}1\rangle$, and $|\frac{5}{2}^{-}1\rangle$ with the width of $\Gamma=3.5$ MeV.

The upper peak at $E_{\Lambda}\sim 13$ MeV corresponds to the state $|\frac{5}{2}^{-}1\rangle$, with the dominant component $|17.5\ \mathrm{MeV},2^{-}1\rangle|s_{\Lambda}\rangle$. The underlying $2^{-}1$ level of ^{6}He has mainly $|^{33}P_{2}[33]\rangle$ structure and forms isospin analog state to the well known one in ^{6}Li. The HY $|\frac{5}{2}^{-}1\rangle$ state is very narrow ($\Gamma\sim 1.5$ MeV), because it lies just above the threshold of the only opened decay channel ($^{4}_{\Lambda}H^{*}+t$). It constitutes a spin doublet partner to the $|\frac{3}{2}^{-}1\rangle$ state discussed in Sec. IV A and thus can serve again as the test of NN interaction used. Moreover, the relative position of the doublet partners $|\frac{3}{2}^{-}1\rangle$ and $|\frac{5}{2}^{-}1\rangle$ [known from combining $(K^{-}\pi^{-})$ and (γ,K^{+}) reactions] constrains strongly the hypernuclear spin-spin interaction.

The splitting of the lowest peak into two may be observed, provided the resolution as good as some 1 MeV is achieved. When increasing the angle θ_{K} (Fig. 10), the above-mentioned states get polarized. The lower $|\frac{1}{2}^{+}1\rangle$ state has $P=-0.33$ and the higher one consists of two states $|\frac{5}{2}^{+}1\rangle+|\frac{3}{2}^{+}1\rangle$ with $P=-0.22+0.13$. The pronounced states in the middle peak possess a higher polarization; in particular $|\frac{3}{2}^{-}1\rangle$ has $P=-0.30$ and $|\frac{7}{2}^{-}1\rangle$ has $P=-0.32$. The main component of the upper peak $|\frac{5}{2}^{-}1\rangle$ has $P=-0.15$ only. There are again many states in the spectrum with higher polarization, but they are excited only very weakly.

For the HY spectroscopy, the reaction $^{7}\mathrm{Li}(\gamma,K^{0})^{7}_{\Lambda}\mathrm{Li}$ would be very useful, and as noted in Refs. 37 and 38, it would be feasible at CEBAF. In this reaction, both isospin branches $T=0,1$ are excited. For $T=0$ case, the complementarity of the photoproduction and $(\pi^{+}K^{+})$ reactions may be used to advantage. In particular (see Fig. 11), there is encountered the strongly excited $|\frac{3}{2}^{+}0\rangle$ state (at $E_{\Lambda}=-4.68$ MeV as obtained here), which is the

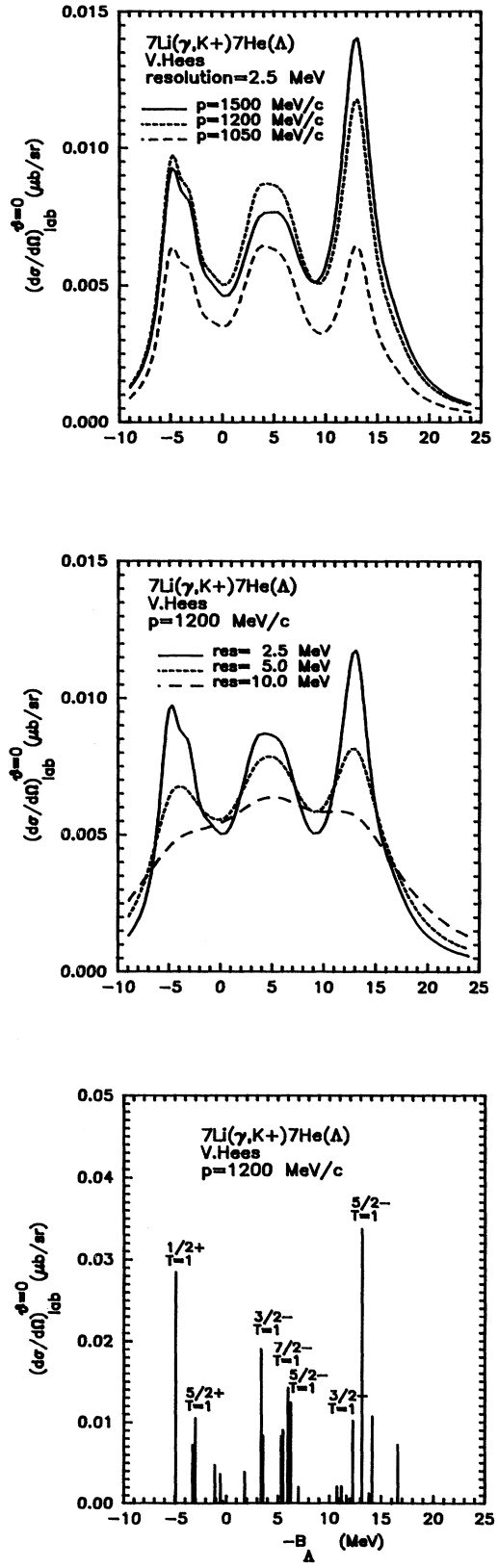

FIG. 9. Photoproduction $^{7}\mathrm{Li}(\gamma,K^{+})^{7}_{\Lambda}\mathrm{He}$ excitation functions at $\theta_K=0°$, various p_γ and resolutions.

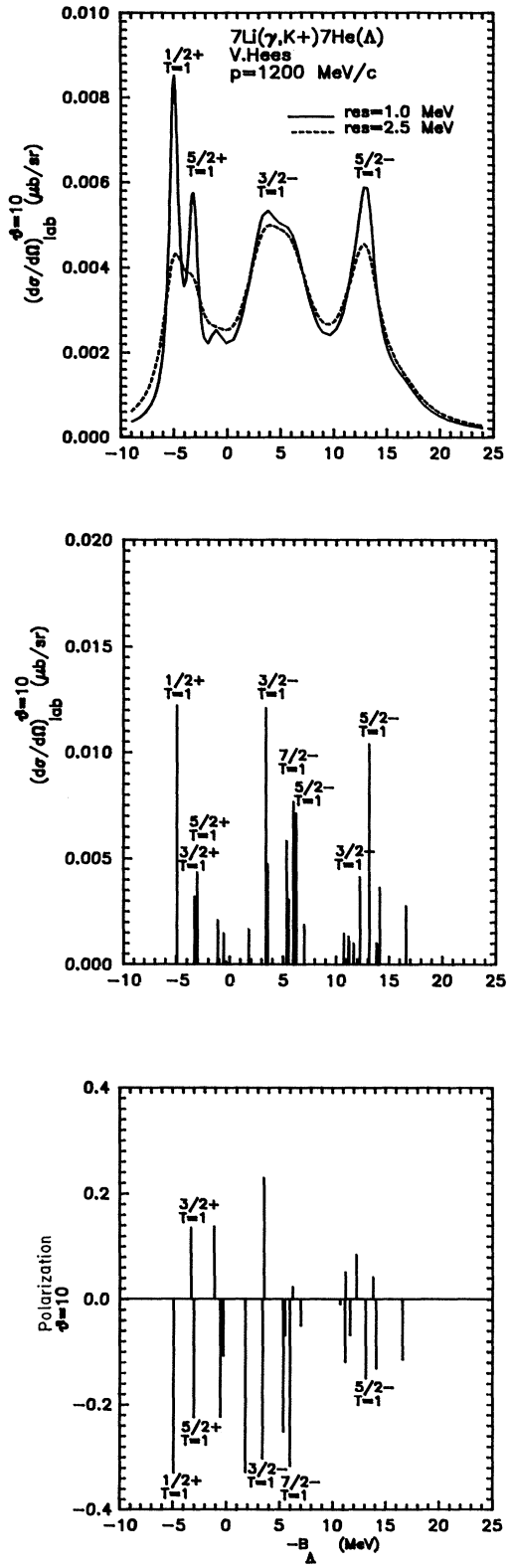

FIG. 10. Photoproduction $^{7}\mathrm{Li}(\gamma,K^{+})^{7}_{\Lambda}\mathrm{He}$ excitation functions and polarization at $p_\gamma=1.2$ GeV/c and $\theta_K=10°$; employed resolutions are 1.0 and 2.5 MeV.

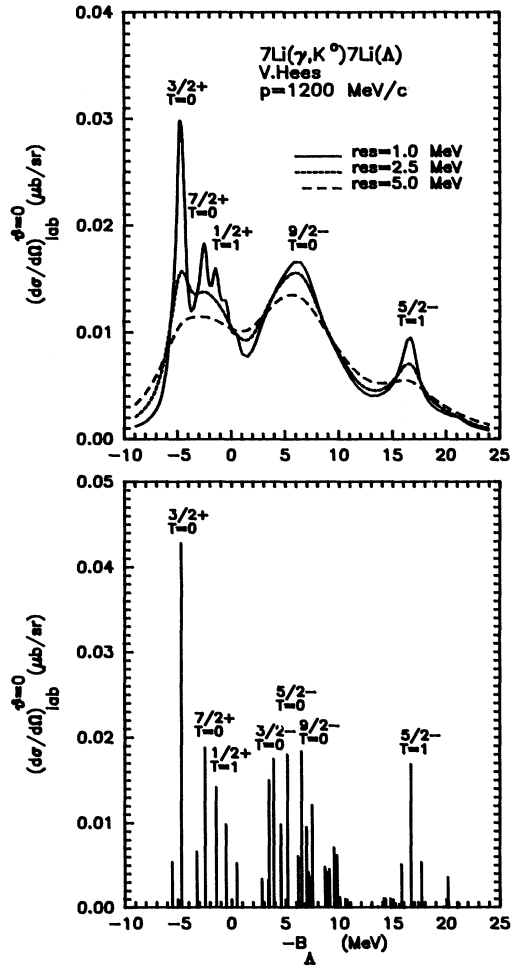

FIG. 11. Schematic estimate (see text) of the photoproduction $^{7}\mathrm{Li}(\gamma,K^{0})^{7}_{\Lambda}\mathrm{Li}$ excitation function at $p_{\gamma}=1.2$ GeV, $\theta_{k}=0°$, and $R=1.0$, 2.5, and 5 MeV.

upper member of the ground-state doublet. The position of this bound state is important for fixing the spin-exchange strength in the effective ΛN interaction.[17] In view of the lack of reliable theoretical and experimental data on the (γ,K^{0}) reaction, the (γ,K^{+}) elementary amplitude was used here instead, for the first rough estimate of the $^{7}_{\Lambda}\mathrm{Li}$ excitation function. The possible differences between both amplitudes are discussed in Ref. 37 and a calculation of the (γ,K^{0}) one is in progress.

V. CONCLUSIONS

The detailed comparison of hypernuclear productions on $^{7}\mathrm{Li}$ pointed not only to specific properties of those reactions, explained by different kinematics, (spin) structure of their transition operators, and response to the nuclear medium. It also revealed a necessity of an increased precision via the resolution reduced below 1 MeV or via the spectroscopy of the secondary HY γ quanta. The polarization experiments may further improve the spectroscopic predictions. All three analyzed reactions excite a variety of states; combination of results allows us to obtain the full HY spectrum and complete doublets. All three reactions are able to polarize substantially some *a priori* known states. For that, a suitable kinematical region is needed, which would optimize the information output. This arises at $\theta\sim 10°$ and at momenta $p_{K}=0.905$ or 1.1 GeV/c for the (K^{-},π^{-}) reaction, $p_{\pi}=1.05$ or 1.5 GeV/c or the (π^{+},K^{+}) reaction, and $p_{\gamma}=1.2$ GeV/c for the (γ,K^{+}) reaction.

The rich spectra of $^{7}_{\Lambda}\mathrm{Li}$ ($^{7}_{\Lambda}\mathrm{He}$)—and for that reason a very involved treatment of the structure was needed—allow us to test not only the ΛN interaction, but also the NN interaction, which controls the reliability of the underlying nuclear core.

It should be noted in passing that the electromagnetic production of strangeness is especially appealing because of the richness of the transition operator, strong population of the low-lying bound states and of complete doublets. In this respect, the electroproduction $(e,e'K^{+})$ may appear more efficient than the photoproduction (γ,K^{+}) due to larger cross sections, larger kinematical flexibility (virtual photons), and a possibility of a better resolution (internal versus extracted electron beams), which is crucial in the hypernuclear spectroscopy, aimed at presently. $^{7}\mathrm{Li}$ will then be a useful target and $^{7}_{\Lambda}\mathrm{Li}$ a distinguishing testing ground.

The discussions, and useful comments by L. Majling, T. Motoba, and S. Frullani, are gratefully acknowledged.

APPENDIX

The transformation of amplitudes from the 2 c.m. system into the two-body laboratory system,

$$A_{j}=\alpha\sum_{i}\lambda_{i}^{j}F_{i}\ , \tag{A1}$$

is described by defining the constants λ_{i}^{j}. They were given previously[20] for (K^{-},π^{-}) and (π^{+},K^{+}) reactions (there $i,j=1,2$) and for the photoproduction $(i,j=1,\ldots,4)$ they read as follows:

$$\lambda_{1}^{1}=(w+m_{N})\left[1-\frac{(w-m_{N})(k_{\gamma}-P_{K}\cos\theta)}{(w+m_{N})(E_{Y}+m_{Y})}\right]\ , \tag{A2}$$

$$\lambda_{2}^{1}=\frac{\varepsilon_{Y}+m_{Y}}{E_{Y}+m_{Y}}[(w+m_{N})(k_{\gamma}-P_{K}\cos\theta) -(w-m_{N})(E_{Y}+m_{Y})]\ , \tag{A3}$$

$$\lambda_{3}^{1}=\lambda_{4}^{1}=0\ , \tag{A4}$$

$$\lambda_{1}^{2}=-P_{K}\frac{w-m_{N}}{E_{Y}+m_{Y}}\ , \tag{A5}$$

$$\lambda_{2}^{2}=(w+m_{N})\frac{\varepsilon_{Y}+m_{Y}}{E_{Y}+m_{Y}}\frac{P_{K}}{q}\ , \tag{A6}$$

$$\lambda_{3}^{2}=\left[w+m_{N}-\frac{k_{\gamma}(w-m_{N})}{E_{Y}+m_{Y}}\right]\frac{P_{K}}{q}\ , \tag{A7}$$

$$\lambda_4^2=\frac{\varepsilon_Y+m_Y}{q}\left[w-m_N-\frac{k_\gamma(w+m_N)}{E_Y+m_Y}\right]\frac{P_K}{q}\ , \tag{A8}$$

$$\lambda_1^3=\lambda_2^3=0\ , \tag{A9}$$

$$\lambda_3^3=\frac{w-m_N}{E_Y+m_Y}\frac{P_K^2}{q}\ , \tag{A10}$$

$$\lambda_4^3=\frac{(w+m_N)(\varepsilon_Y+m_Y)}{E_Y+m_Y}\frac{P_K^2}{q^2}\ , \tag{A11}$$

$$\lambda_1^4=\frac{w-m_N}{E_Y+m_Y}P_K\ , \tag{A12}$$

$$\lambda_2^4=-\frac{(w+m_N)(\varepsilon_Y+m_Y)}{E_Y+m_Y}\frac{P_K}{q}\ , \tag{A13}$$

$$\lambda_3^4=\lambda_4^4=0\ , \tag{A14}$$

where

$$\alpha=\frac{1}{2w(w-m_N)}\left[\frac{2k_\gamma(E_Y+m_Y)}{E_KE_Y(\varepsilon_N+m_N)(\varepsilon_Y+m_Y)}\right]^{1/2}\ ,$$

$$w=\sqrt{s}\equiv\varepsilon_\gamma+\varepsilon_N\ ,$$

ε are 2 c.m. energies [$\varepsilon_N=\sqrt{m_N^2+\kappa^2}$, $\varepsilon_Y=\sqrt{m_Y^2+q^2}$, $\varepsilon_\gamma=\kappa$], κ and q are 2 c.m. in an out momenta, E are two-body laboratory energies [$E_Y=\sqrt{m_Y^2+(\mathbf{k}_\gamma-\mathbf{P}_K)^2}$, $E_K=\sqrt{m_K^2+P_K^2}$], and k_γ and P_κ are two-body laboratory momenta.

[1]R. Bertini *et al.*, Nucl. Phys. **A368**, 365 (1981); **A360**, 315 (1981).

[2]T. Motoba, H. Bando. K. Ikeda, and T. Yamada, Prog. Theor. Phys. Suppl. **81**, 42 (1985).

[3]H. Bando, T. Motoba, M. Sotona, and J. Žofka, Phys. Rev. C **39**, 587 (1989).

[4]A. S. Rosenthal, D. Halderson, K. Hodgkinson, and F. Tabakin, Ann. Phys. (N.Y.) **184**, 33 (1988).

[5]M. Sotona and J. Žofka, Czech. J. Phys. B **40**, 1091 (1990).

[6]G. P. Gopal, R. T. Ross, A. J. Van Horn, A. C. McPherson, E. F. Clayton, T. C. Bacon, and I. Butterworth, Nucl. Phys. **B119**, 362 (1977).

[7]M. Sotona and J. Žofka, Prog. Theor. Phys. **81**, 160 (1989).

[8]L. Majling, M. Sotona, J. Žofka, V. N. Fetisov, and R. A. Eramzhyan, Phys. Lett. **92B**, 256 (1980).

[9]A. G. M. van Hees and P. W. M. Glaudemans, Z. Phys. A **314**, 323 (1983).

[10]H. de Vries *et al.*, At. Data Nucl. Data Tables **36**, 495 (1987).

[11]T. W. Donelly and J. D. Walecka, Phys. Lett. **44B**, 330 (1973).

[12]F. C. Barker, Nucl. Phys. **83**, 418 (1966).

[13]E. H. Auerbach, A. J. Baltz, C. B. Dover, A. Gal, S. H. Kahana, L. Ludeking, and D. J. Millener, Ann. Phys. (N.Y.) **148**, 318 (1983).

[14]O. Richter, in *Contributed Papers of XI Few Body Systems in Particle and Nuclear Physics, Tokyo, 1986,* edited by T. Sasakawa *et al.* (Tohoku University, Sendai, 1986), p. 206.

[15]D. Halderson, Phys. Rev. C **30**, 941 (1984).

[16]A. Gal, J. M. Soper, and R. H. Dalitz, Ann. Phys. (N.Y.) **63**, 53 (1971).

[17]D. J. Millener, A. Gal, C. B. Dover, and R. H. Dalitz, Phys. Rev. C **31**, 499 (1985).

[18]R. E. Chrien *et al.*, Phys. Rev. C **41**, 1062 (1990).

[19]L. Majling, J. Žofka, V. N. Fetisov, and R. A. Eramzhyan, Institute for Nuclear Study Report INS-Rep.-810, Tokyo, 1990.

[20]M. Sotona, J. Žofka, V. N. Fetisov, and H. Bando, Czech, J. Phys. B **39**, 1273 (1989).

[21]H. Bando, T. Motoba, and J. Žofka, Int. J. Mod. Phys. A **5**, 4021 (1990).

[22]T. Motoba, H. Bando, R. Wünsch, and J. Žofka, Phys. Rev. C **38**, 1322 (1988).

[23]V. N. Fetisov, M. I. Kozlov, and A. I. Lebedev, Phys. Lett. **38B**, 129 (1972).

[24]A. M. Bernstein, T. W. Donnelly, and G. N. Epstein, Nucl. Phys. **A358**, 195c (1981).

[25]S. S. Hsiao and S. R. Cotanch, Phys. Rev. C **28**, 1668 (1983); Nucl. Phys. **A450**, 419c (1986).

[26]J. Cohen, M. W. Price, and G. E. Walker, Phys. Lett. B **188**, 393 (1987); J. Cohen, Phys. Rev. C **32**, 543 (1985); Phys. Lett. **153B**, 367 (1985); Phys. Lett. B **192**, 291 (1987).

[27]H. Tanabe, M. Kohno, and C. Bennhold, Phys. Rev. C **39**, 741 (1989); C. Bennhold and L. E. Wright, *ibid.* **36**, 438 (1987); Phys. Lett. B **191**, 11 (1987).

[28]W. Schorsch, J. Tietge, and W. Weilnböck, Nucl. Phys. **B25**, 179 (1970).

[29]C. Bennhold, Institut für Kernphysik Report MUPH-T-89-15, Mainz, 1989.

[30]H. A. Grunder, in *4th Workshop on Perspectives in Nuclear Physics at Intermediate Energies, Trieste, 1989,* edited by S. Boffi *et al.* (World Scientific, Singapore, 1989), p. 210.

[31]T. Motoba, H. Bando, and K. Ikeda, Prog. Theor. Phys. **70**, 189 (1983).

[32]V. A. Knyr, A. I. Mazur, and Yu. F. Smirnov, in *Supplementary Proceedings of the III International Conference on Mesons and Light Nuclei, Bechyně, 1985,* edited by R. Mach *et al.* (TSV, Bechyně, 1986), p. 27.

[33]R. A. Eramzhyan, T. D. Kaipov, and S. S. Kamalov, Z. Phys. A **322**, 321 (1985).

[34]M. May *et al.*, Phys. Rev. Lett. **51**, 2085 (1983).

[35]T. Kishimoto, H. Ejiri, and H. Bando, Phys. Lett. **232B**, 24 (1989).

[36]H. Bando, Suppl. J. Phys. Soc. Jpn. **58**, 379 (1989).

[37]C. B. Dover and D. J. Millener, BNL Report 44651, 1990.

[38]J. Berthot and P. Y. Bertin, in *Research Program at CEBAF (III)* (CEBAF, Newport News, 1987), p. 406.